RUNX1 transactivates *BCR-ABL1* expression in Philadelphia chromosome positive acute lymphoblastic leukemia

（RUNX1 はフィラデルフィア染色体陽性急性リンパ性白血病において *BCR-ABL1* の発現を転写制御する）

増田　達哉

ORIGINAL ARTICLE

RUNX1 transactivates *BCR-ABL1* expression in Philadelphia chromosome positive acute lymphoblastic leukemia

Tatsuya Masuda[1] | Shintaro Maeda[1] | Sae Shimada[1] | Naoya Sakuramoto[1] | Ken Morita[1] | Asami Koyama[1] | Kensho Suzuki[1] | Yoshihide Mitsuda[1] | Hidemasa Matsuo[1] | Hirohito Kubota[2] | Itaru Kato[2] | Kuniaki Tanaka[2] | Junko Takita[2] | Masahiro Hirata[3] | Tatsuki R Kataoka[3] | Tatsutoshi Nakahata[4] | Souichi Adachi[1] | Hideyo Hirai[5] | Shuichi Mizuta[6] | Kazuhito Naka[7] | Yoichi Imai[8] | Shinya Kimura[9] | Hiroshi Sugiyama[10] | Yasuhiko Kamikubo[1]

[1]Department of Human Health Sciences, Graduate School of Medicine, Kyoto University, Kyoto, Japan

[2]Department of Pediatrics, Graduate School of Medicine, Kyoto University, Kyoto, Japan

[3]Department of Diagnostic Pathology, Kyoto University Hospital, Kyoto, Japan

[4]Department of Clinical Application, Center for iPS Cell Research and Application, Kyoto University, Kyoto, Japan

[5]Department of Transfusion Medicine and Cell Therapy, Kyoto University Hospital, Kyoto, Japan

[6]Hematology & Immunology, Kanazawa Medical University, Uchinada, Kahoku-gun, Japan

[7]Research Institute for Radiation Biology and Medicine, Hiroshima University, Hiroshima, Japan

[8]Department of Hematology/Oncology, IMSUT Hospital, The Institute of Medical Science, The University of Tokyo, Tokyo, Japan

[9]Faculty of Medicine, Division of Hematology, Respiratory Medicine and Oncology, Department of Internal Medicine, Saga University, Saga, Japan

[10]Department of Chemistry, Graduate School of Science, Kyoto University, Kyoto, Japan

Correspondence
Hiroshi Sugiyama, Department of Chemistry, Graduate School of Science, Kyoto University, Sakyo-ku, Kyoto 606-8502, Japan.
Email: hs@kuchem.kyoto-u.ac.jp

Yasuhiko Kamikubo, Human Health Sciences, Graduate School of Medicine, Kyoto University, 53 Kawahara-cho, Syogoin, Sakyo-ku, Kyoto 606-8507, Japan.
Email: kamikubo.yasuhiko.7u@kyoto-u.ac.jp

Abstract

The emergence of tyrosine kinase inhibitors as part of a front-line treatment has greatly improved the clinical outcome of the patients with Ph$^+$ acute lymphoblastic leukemia (ALL). However, a portion of them still become refractory to the therapy mainly through acquiring mutations in the *BCR-ABL1* gene, necessitating a novel strategy to treat tyrosine kinase inhibitor (TKI)-resistant Ph$^+$ ALL cases. In this report, we show evidence that RUNX1 transcription factor stringently controls the expression of *BCR-ABL1*, which can strategically be targeted by our novel RUNX inhibitor, Chb-M'. Through a series of in vitro experiments, we identified that RUNX1 binds to the promoter of *BCR* and directly transactivates *BCR-ABL1* expression in Ph$^+$ ALL cell lines. These cells showed significantly reduced expression of *BCR-ABL1* with suppressed proliferation upon *RUNX1* knockdown. Moreover, treatment with Chb-M' consistently downregulated the expression of *BCR-ABL1* in these cells and this drug was highly

effective even in an imatinib-resistant Ph⁺ ALL cell line. In good agreement with these findings, forced expression of *BCR-ABL1* in these cells conferred relative resistance to Chb-M'. In addition, in vivo experiments with the Ph⁺ ALL patient-derived xenograft cells showed similar results. In summary, targeting RUNX1 therapeutically in Ph⁺ ALL cells may lead to overcoming TKI resistance through the transcriptional regulation of *BCR-ABL1*. Chb-M' could be a novel drug for patients with TKI-resistant refractory Ph⁺ ALL.

KEYWORDS
bcr-abl, fusion proteins, gene expression regulation, leukemia, lymphoid, Philadelphia chromosome, RUNX1 protein, human

1 | INTRODUCTION

Acute lymphoblastic leukemia (ALL) is an acute form of leukemia characterized by the emergence of highly proliferative immature white blood cells, known as lymphoblasts. Approximately 6000 new cases are reported yearly in the United States and ALL is the most frequently encountered malignancy in childhood.[1-3] ALL is one of the first cancers for which an effective chemotherapeutic treatment was developed and its cure is now a realistic goal and is achieved in more than 90% of affected children,[3-6] while only 20%-40% of adults respond to and survive courses of intensified chemotherapies.[7,8] This difference is supposed to originate from the vulnerability of elderly patients who have weakened immune and circulatory organ systems. Philadelphia chromosome positive ALL (Ph⁺ ALL) marks a subset of leukemia with distinctive treatment strategy and outcomes due to the existence of the *BCR-ABL1* pathogenic fusion gene that is created by juxtaposing the *ABL1* gene on chromosome 9 to part of the *BCR* gene on chromosome 22.[3,9] The emergence of imatinib mesylate, a tyrosine kinase inhibitor (TKI) that inhibits ABL1, KIT and PDGFR, entirely changed the game of anti-leukemia strategy toward Ph⁺ ALL.[10,11] Adding imatinib to standard therapy improved the outcomes for adults with Ph⁺ ALL, at least in part, by facilitating allogeneic stem cell transplant.[12] However, a portion of adults steadily develop resistance to TKI therapy, mainly through acquiring point mutations in the kinase domain of *BCR-ABL1* in ALL cells.[13] These patients can be treated by the next generation of tyrosine kinase inhibitors such as nilotinib, dasatinib, or ponatinib. In particular, the third-generation TKI, ponatinib, is a potent orally bioavailable pan BCR-ABL1 inhibitor that inhibits both wild-type and mutant BCR-ABL1 kinase, including the "gatekeeper" T315I mutation, which is resistant to all other currently available TKIs.[14,15] However, because of the risk of cardiovascular side effects, the risk/benefit balance must be evaluated for each patient.[14] Therefore, a new treatment modality against TKI treatment-resistant Ph⁺ ALL with no side effects is highly needed.

Runt-related transcription factor 1 (RUNX1), also known as acute myeloid leukemia 1 protein (AML1), is an essential master transcription factor implicated in the differentiation and the maintenance of hematopoietic stem cells.[16] In ALL, a well known t(12;21)(p13.1;q22) translocation causes the fusion of the ETS variant 6 (*ETV6*) and RUNX1 genes (*ETV6-RUNX1*, formerly *TEL-AML1*). It is the most common translocation in childhood ALL,[17] suggesting a fundamental involvement of RUNX1 in the pathogenesis of a subset of ALL cases. Intriguingly, Yamamoto K et.al.[18] reported that the elevated expressions of wild-type RUNX1 closely correlates with worse outcomes in chronic myeloid leukemia (CML) patients, another type of leukemia caused by the same chimeric protein BCR-ABL1 as Ph⁺ ALL but with a different break point. The molecular mechanisms underlying the possible interaction of *RUNX1* and *BCR-ABL1*, however, have poorly been elucidated so far. We have previously reported the requirement of RUNX1 in the development and the maintenance of AML,[19-24] another form of acute leukemia originating in myeloid progenitor cells. In this report, we addressed the leukemogenic role of RUNX1 in Ph⁺ ALL and elaborated to elucidate the molecular mechanisms in the regulation of *BCR-ABL1* expression and in the proliferation of Ph⁺ leukemia cells.

2 | MATERIALS AND METHODS

2.1 | Cell lines and plasmids

SU-Ph2 is an imatinib-sensitive cell line established from a patient with Ph⁺ALL. SU/SR is an imatinib-resistant subline of SU-Ph2 obtained after long-term exposure to imatinib until they finally acquired the T315I mutation in *BCR-ABL1* gene. These cells were kindly gifted from Dr. A. Kanamaru (Department of Internal Medicine, Kinki University School of Medicine, Osaka, Japan). ALL-derived BALL-1, KOCL-45, SUP-B15, SU-Ph2 and SU/SR cells as well as CML-derived MYL, BV173 and K562 cells were maintained in RPMI 1640 medium with 10% heat-inactivated FBS and 1% penicillin-streptomycin at 37°C in 5% CO_2.

Human *BCR-ABL1* was a kind gift from Nora Heisterkamp (Addgene plasmid # 31 285). pENTR1A Dual Selection vector (Thermo Fisher Scientific), CSIV-TRE-RfA-UbC-KT and CSII-EF-MCS-IRES-hKO1 (RIKEN BRC) were used to construct expression vectors. All of the products were verified by DNA sequencing.

2.2 | Dual luciferase reporter assay

HEK293T cells were seeded in 10 mL DMEM supplemented with 10% heat-inactivated FBS and 1% PS 1 d before transfection. Cells were transfected with 10 μg of pGL4.20 harboring the *BCR* promoter and 1 μg pRL-CMV with polyethylenimine (PEI; Sigma-Aldrich). The *BCR* promoter region was amplified from the genomic DNA of SU/SR cells using specific primers (F 5′-TTAGAGGGAGGCTAATCAGGG-3′ and R 5′-TCCTCGGACGCTAAGCTC-3′). At 24 h after transfection, doxycycline was added at 3 μmol L^{-1} and incubated for another 24 h. The cells were then rinsed twice with PBS and lysed with 1× lysis buffer as supplied in the PicaGene® Dual Sea Pansy Luminescence kit (TOYO B-net). The luciferase and Renilla luciferase activity were measured using ARVO X5 (PerkinElmer).

2.3 | IC$_{50}$ evaluation

For cell survival assay, 3×10^4 cells were seeded onto 96-well flat plates. The indicated concentrations of PI polyamides or drugs were added to the culture medium and cells were incubated for 48 h. Cell viability was then assessed using the Cell Count Reagent SF (nacalai tesque, Inc) and the Infinite® 200 PRO multimode reader (TECAN). Percent inhibition curves were drawn and IC$_{50}$ of the indicated compounds was calculated based on median-effect method.[25]

2.4 | Statistics

Statistical significance of differences between control and experimental groups was assessed using a 2-tailed unpaired Student *t* test and was declared if the *P*-value was less than .05. Equality of variances in 2 populations was calculated using the *F* test. The results were represented as the average ± SD values obtained from 3 independent experiments.

2.5 | Quantitative RT-PCR

Quantitative RT-PCR (qRT-PCR) was conducted as previously described.[26] Briefly, total RNA was extracted from cultured cells using the RNeasy mini kit (Quiagen) and reverse transcribed using the ReverTra Ace® qPCR RT Master Mix (TOYOBO) to generate cDNA. qRT-PCR was conducted on the StepOne™ real-time PCR system (Applied Biosystems). Relative expression levels were calculated using the $2^{-\Delta\Delta Ct}$ method. Primers used for qRT-PCR are listed in Table S1.

2.6 | ChIP-PCR

ChIP assay was performed using SimpleChIP® Plus enzymatic Chromatin IP Kit (Cell Signaling Technology) according to the manufacturer's instructions. Chromatin preparation was processed for immunoprecipitation with anti-RUNX1 antibody (ab23980, abcam) at 4°C overnight. Following ChIP, DNA was amplified with specific primers listed in Table S2 using Ex *Taq*® polymerase (Takara Bio Inc). Obtained DNA was analyzed using agarose gel electrophoresis.

2.7 | Immunoblotting

Cells were washed twice in ice-cold PBS and lysed in lysis buffer as previously described.[21] Equal amounts of protein samples were loaded onto the gels for each target proteins, separated using SDS-PAGE and electrotransferred onto 45-μm pore size polyvinylidene difluoride membranes (Millipore, IPVH00010). Membranes were probed with the following primary antibodies: anti-c-abl (Cell Signaling Technology, 2862), anti-RUNX1 (Santa Cruz Biotechnology, clone A-2), anti-GAPDH (Santa Cruz Biotechnology, clone 0411), anti-phospho-AKT(Ser473; Cell Signaling Technology, 9271), anti-AKT (Cell Signaling Technology, 9272) and anti-p53 (Santa Cruz Biotechnology, clone DO-1) antibodies. For secondary antibodies, HRP-conjugated anti-rabbit IgG and anti-mouse IgG (Cell Signaling Technology, 7074 and 7076) were used. Primary antibodies and secondary antibodies were diluted to 1:1000 and 1:5000. Blots were visualized using Chemi-Lumi One Super (Nacalai Tesque) and the ChemiDoc XRS + Imager (Bio-Rad Laboratories).

2.8 | shRNA interference

shRNA targeting human *RUNX1*, *BCR-ABL1*, and *p53* were designed and sub-cloned into pENTR4-H1tetOx1, CS-RfA-ETV, CS-RfA-ETBsd vectors (RIKEN BRC). Non-targeting control shRNA was designed against *luciferase* (sh_*Luc*). The target sequences were provided in Table S3.

2.9 | Xenograft mouse model

NOD/Shi-scid, IL-2RγKO (NOG) mice were purchased from the Central Institute for Experimental Animals, Japan and were used as controls in all experiments. For leukemia cell lines mouse xenograft models, 2×10^6 cells/body of SU/SR cells with doxycycline-inducible shRNA expression vector targeting *Luciferase* or *RUNX1* were injected intravenously into NOG mice. At 7 d after transplantation, 1 mg/mL doxycycline (Sigma) and 30 mg/mL sucrose (Wako) were added to the drinking water and started to be given orally. Peripheral blood was then collected every week and chimerism was checked by a flow cytometer. For the patient-derived xenograft (PDX) study, PDX cells were provided by Dr. Itaru Kato's group. Appropriate informed consent was obtained from this patient. At the age of 6, she was diagnosed with Ph1-positive BCP-ALL (minor *BCR-ABL1*-positive), and was in remission with multidrug chemotherapy including imatinib. At 1 y and 6 mo

after the diagnosis, she had a isolated central nervous system (CNS) recurrence. She achieved remission again after switching to dasatinib, Hyper-CVAD, and intensified intrathecal injections. Bone marrow transplantation was performed from an HLA-matched relative donor, but she had the second relapse in the CNS. At the second CNS recurrence, the T315I mutation was tested and was negative. She became refractory to treatment and died 1 y and 4 mo after transplantation. The PDX cells used in this study were established using leukemia cells collected from cerebrospinal fluid at the time of the first relapse of the CNS alone. These PDX cells were intravenously transplanted into NOG mice. At 2 wk after transplantation, Chb-M' (320 µg/kg body weight, twice per week) or DMSO (the equivalent amount, twice per week) administration was intravenously started, and oral administration of imatinib mesylate (Tokyo Chemical Industry Co., Ltd., 100 mg/kg body weight, daily) was started. Bone marrow was then collected every week and chimerism was checked using a flow cytometer and an anti-human CD45 antibody and an anti-mouse CD45 antibody (BD Biosciences). Overall survival was monitored until the mice succumbed to their disease. For the bone marrow of 1 representative of each group at day 36, H&E staining and immunohistochemical staining with anti-human CD45 antibody (Thermo Fisher Scientific, MA5-13197), anti-Ki-67 antibody (Agilent, M7240), anti-RUNX1 antibody (Abcam, ab35962) and anti-BCR (BCR-ABL1 p190/p210) antibody (Santa Cruz Biotechnology, G6) were done.

2.10 | Study approval

All animal studies were properly conducted according to the Regulations on Animal Experimentation at Kyoto University, based on International Guiding Principles for Biomedical Research Involving Animals. All procedures used in this study were approved by the Kyoto University Animal Experimentation Committee (Permit Number: Med Kyo 14 332). PDX analysis was approved by the Kyoto University Hospital Ethical Board (Approval number: G-1030).

3 | RESULTS

3.1 | Knockdown of *RUNX1* suppresses the proliferation of Ph$^+$ ALL cell lines

To explore the role of RUNX1 in the maintenance of Ph$^+$ ALL cells, we first modulated the expression of *RUNX1* in human Ph$^+$ ALL-derived

SU/SR cells with doxycycline-inducible shRNA. SU/SR cells are genetically identical to SU-Ph2 cells except for the T315I point mutation in the ABL1 protein, which confers major resistance to TKI treatment (Figure S1).[27-30] As shown in Figure 1A,B, silencing of *RUNX1* significantly suppressed the cell growth of SU/SR imatinib-resistant Ph$^+$ ALL cells in vitro. Intriguingly, this *RUNX1* inhibition-mediated suppression of tumor growth was observed not only in Ph$^+$ ALL-derived SU/SR and SU/Ph2 cells, but also in CML-derived MYL and K562 cells (Figure S2). As widely known, while *BCR-ABL1* p190 occurs in the majority of Ph$^+$ ALL cases, *BCR-ABL1* p210 is the hallmark of CML, and both fusion genes are thought to be under the control of the *BCR* promoter. These results prompted us to further investigate the role of RUNX1 in *BCR-ABL1*-dependent hematologic malignancies.

We next investigated the effect of *RUNX1* inhibition in Ph$^+$ ALL cells in vivo, and prepared a Ph$^+$ ALL xenograft model. We transplanted SU/SR cells that had been stably transduced with lentivirus expressing control sh_*Luc* or sh_*RUNX1* into immunodeficient NOG mice. At 7 d after the transplantation, doxycycline administration was started to induce in vivo *RUNX1* knockdown (Figure 1C). Peripheral blood was collected every week to check the chimerism of transplanted ALL cells (Figure 1D). Overall survival periods were monitored until they succumbed to their disease. Thoroughly consistent with the results observed in the in vitro experiments, NOG mice transplanted with *RUNX1*-silenced SU/SR cells exhibited prolonged survival with statistical significance (Figure 1E). These mice showed lessened tumor burdens in the spleen and the bone marrow relative to the control (Figure 1F-H).

3.2 | RUNX1 directly transactivates the expression of *BCR-ABL1*

As we found that RUNX1 expression is a prerequisite for the proliferation of Ph$^+$ ALL cell lines, we assumed that its expression might be elevated in Ph$^+$ ALL patients. As shown in Figure 2A, analysis of a microarray dataset elucidated that the expression of *RUNX1* indeed increased in the bone marrow cells and peripheral blood cells derived from Ph$^+$ ALL patients relative to those from the healthy donors and non-leukemic patients. In this data set (GSE13204), non-leukemic patients included those with megaloblastic anemia, hemolysis, iron deficiency, or idiopathic thrombocytopenic purpura. As the expression of the oncogenic *BCR-ABL1* fusion gene is regulated under the *BCR* promoter, as we have mentioned, this finding led us to hypothesize that the expression of the *BCR-ABL1* fusion gene might be transcriptionally controlled by RUNX1.

FIGURE 1 The expression of RUNX1 is required in the maintenance of Ph$^+$ ALL cells. A, Cell growth curves of SU/SR cells transduced with shRNAs targeting *RUNX1* (sh_*RUNX1* #1 and sh_*RUNX1* #2) or *luciferase* (sh_*Luc*). B, Immunoblot of RUNX1 and GAPDH in SU/SR cells transfected with sh_*Luc*, sh_*RUNX1* #1 and sh_*RUNX1* #2. Cells were treated with 3 µmol L^{-1} doxycycline for 24 h. C, Schema of xenotransplantation assay in NOG mice with SU/SR cells (sh_*Luc* or sh_*RUNX1#1*). D, Chimerism of transplanted leukemia cells in (C; n = 5). E, Overall survival of NOG mice in (C; n = 11). F, G, Organ images of the livers (F) and the spleens (G) with the weight boxplots at day 40 in (C; n = 5). H, Representative histology pictures of the bone marrow at day 40 in (C). H&E staining and immunohistochemical staining with anti-human CD45 antibody were done for each slide (original magnification; ×10 (upper panels) and ×40 (lower panels), Scale bars; 200 µm). Mean ± SD. *P < .05, **P < .01, ***P < .001, using two-tailed Student t test (A, D), log-rank (E), Mann-Whitney U test (F, G)
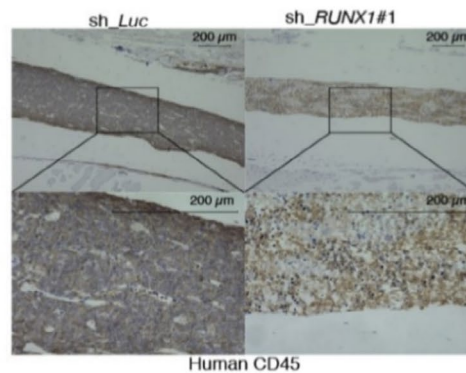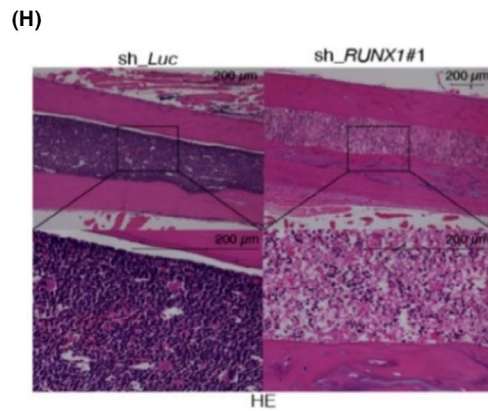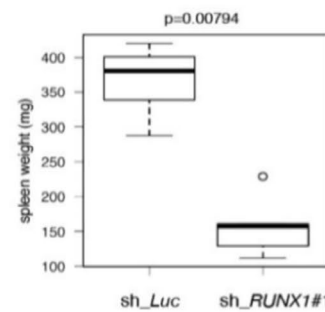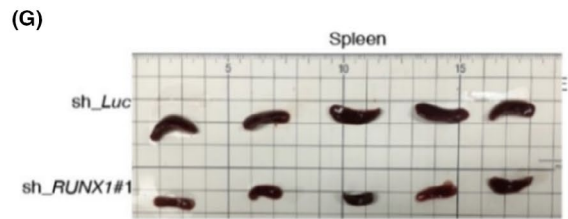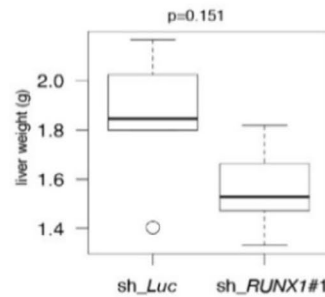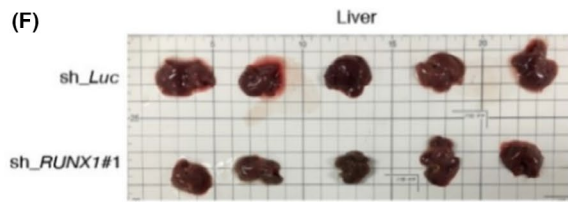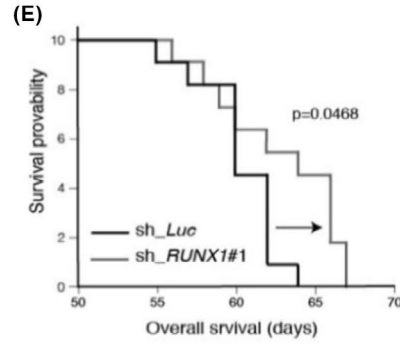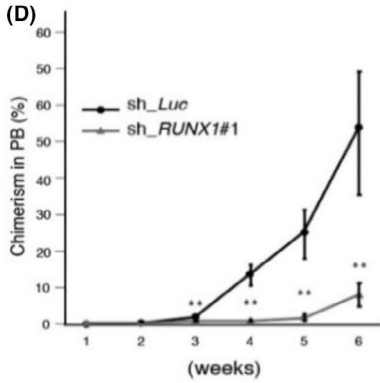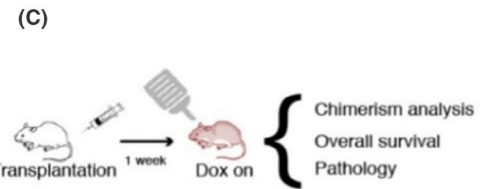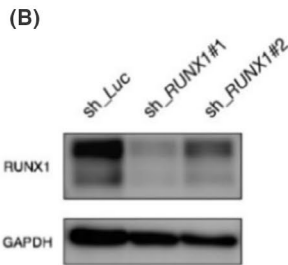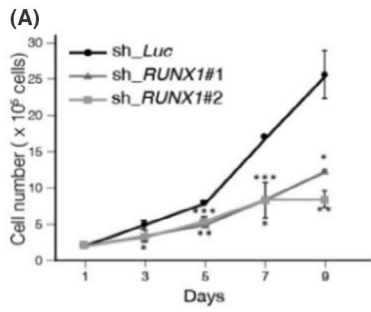
To test our hypothesis, we first examined the expression of *BCR-ABL1* upon *RUNX1* knockdown in SU/SR cells. As shown in Figure 2B,C, the expression of *BCR-ABL1* was significantly downregulated in *RUNX1*-silenced SU/SR cells relative to the control both at mRNA and protein levels. In addition, the phosphorylation level of AKT, one of the most important downstream targets of BCR-ABL1, was also significantly reduced upon knockdown of *RUNX1* in SU/SR cells (Figure 2C). Of note, the growth rate of SU/SR cells was attenuated upon *BCR-ABL1* knockdown to the extent of *RUNX1*-silencing, underpinning the importance of RUNX1 in the regulation of *BCR-ABL1* expression (Figure S3). To address whether RUNX1 directly transactivates *BCR-ABL1* expression, we next conducted luciferase reporter assays using the *BCR* promoter in HEK293T cells. We prepared HEK293T cells that were stably transduced with shRNAs targeting *RUNX1* or lentivirus expressing *RUNX1*. These cells were transiently transfected with a vector harboring a luciferase reporter fused to the *BCR* promoter (located at −1000 to +200 bp relative to the transcription start site [TSS] of *BCR* gene), and the expression

of shRNAs or *RUNX1* was induced by doxycycline. As shown in Figure 2D, while inhibition of *RUNX1* downregulated the activity of the *BCR* promoter, additional *RUNX1* expression consistently upregulated its activity. Close inspection of the *BCR* promoter uncovered the RUNX1 consensus binding site of 5′-TGTGGT-3′ at 802 bp upstream of the TSS of *BCR*. ChIP experiments confirmed the actual binding of RUNX1 in this region (Figure 2E). These results collectively suggested that RUNX1 binds to the promoter of *BCR-ABL1* in Ph⁺ ALL cells and positively regulates it, which could potentially be targeted in anti-leukemia therapy toward this cancer.

3.3 | Novel RUNX inhibitor, Chb-M', induces Ph⁺ALL cell death *BCR-ABL1*-dependently

To further investigate the role of RUNX1 in Ph⁺ALL cells, we next pharmacologically inhibited RUNX1 by our novel RUNX inhibitor Chb-M'[21] and examined its anti-leukemia effect on Ph⁺ ALL cells.
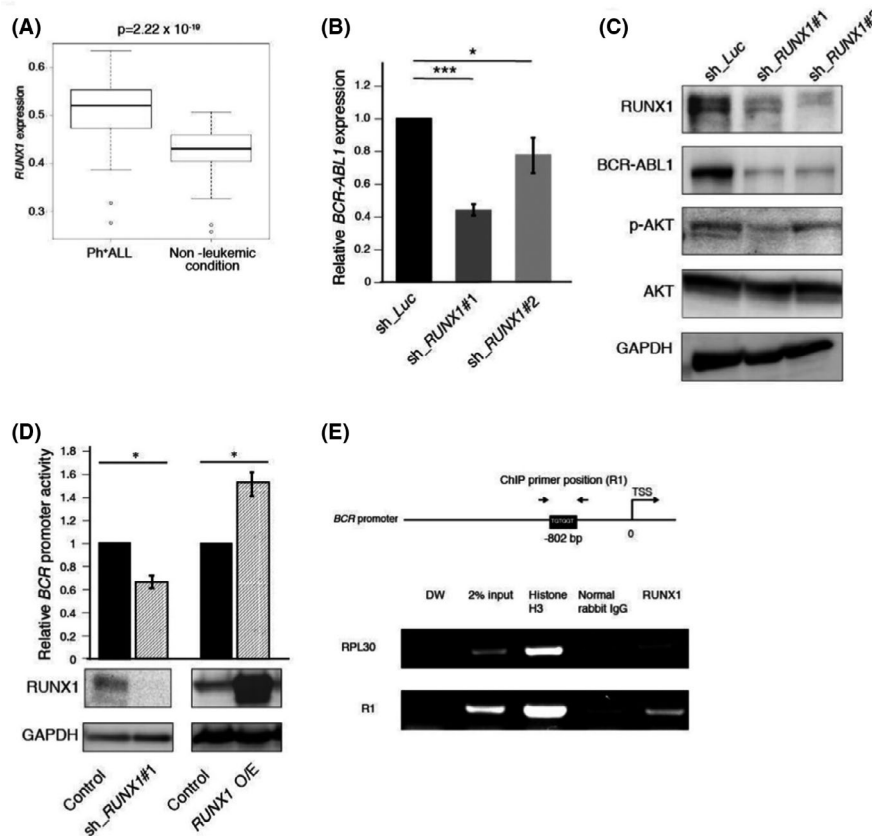
FIGURE 2 R Runt-related transcription factor 1 (RUNX1) directly transactivates the expression of *BCR-ABL1*. A, *RUNX1* expression (probe ID:209360_s_at., GSE13204) in pediatric Ph⁺ ALL (mean = 0.5123, n = 122) and in the control samples (mean = 0.4278, n = 79). B, Relative mRNA expression of *BCR-ABL1* in SU/SR cells stably transduced with sh_*Luc*, sh_*RUNX1* #1 or sh_*RUNX1* #2. Cells were treated with 3 μmol L⁻¹ doxycycline for 24 h. C, Immunoblot of RUNX1, BCR-ABL1, phosphorylated-AKT (p-AKT), AKT and GAPDH in the same SU/SR cells as (B). Cells were treated with 3 μmol L⁻¹ doxycycline for 24 h, then lysed for protein extraction. D, Luciferase reporter activity of *BCR* promoter in HEK293T cells upon knockdown (sh_*RUNX1*#1) or overexpression (*RUNX1* O/E) of *RUNX1* with immunoblot images of RUNX1 and GAPDH in the samples. E, Gel image of ChIP-PCR in SU/SR cells with RUNX1 antibody. The binding of RUNX1 transcription factors to the *BCR* promoter was assessed with the primers amplifying the region including the RUNX1 consensus binding site (5′-TGTGGT-3′) located at 802 bp upstream of TSS (R1). RPL30 was used as RUNX1-irrelevant negative control. Mean ± SD. *P < .05, ***P < .001, using Mann-Whitney *U* test (A), two-tailed Student *t* test (B, D)

Chb-M' is a pyrrole-imidazole polyamide interlocked with a hairpin conjugated with alkylating reagent chlorambucil that specifically recognizes DNA sequences containing 5'-TGTGGT-3', a canonical RUNX1 recognition site. To start with, we examined the specificity of the pyrrole-imidazole polyamide to the 5'-TGTGGT-3' region in the *BCR* promoter by ChIP assay. For this purpose, we prepared alkylating agent-free Chb-M' (Simple-M') and tested whether the binding of RUNX1 to the 5'-TGTGGT-3' site in the *BCR* promoter was competitively inhibited by adding Simple-M'. As shown in Figure 3A, Simple-M' apparently removed RUNX1 from the *BCR* promoter in our ChIP experiment dose dependently.

With respect to the antitumor effect on Ph$^+$ ALL cells, Chb-M' effectively controlled their proliferation in several Ph$^+$ ALL cell lines that we tested in this study (Figure 3B, Figure S4A-D). Furthermore, treatment with Chb-M' downregulated the expression of *BCR-ABL1* both at mRNA and protein levels in these cells (Figures 3C,D and S4E-H). Contrary to Figure 3A, Chb-M' suppressed *BCR-ABL1* expression at lower concentration, suggesting that DNA alkylation by chlorambucil is important for transcriptional regulation, as described in our previous reports.[31,32] The phosphorylation of AKT was also consistently reduced in SU/SR cells upon Chb-M' treatment (Figure 3D). These results were thoroughly consistent with those obtained in the *RUNX1* knockdown experiments. Of note, additional *BCR-ABL1* expression in SU/SR cells and MYL conferred relative resistance to Chb-M' treatment (Figures 3E,F and S5). Moreover, we found that Chb-M' preferentially suppresses the growth of ALL cells with *BCR-ABL1* relative to those without it (Figure 3G). These results collectively suggested that the anti-leukemia effect of Chb-M' largely depended on this oncogenic fusion gene.

We have previously found and reported that the growth suppression induced by Chb-M' is highly dependent on the p53 cell death pathway.[21] Therefore, we tested whether p53 significantly contributed to the Chb-M'-mediated growth suppression in SU/SR cells. For this purpose, we prepared *p53*-knocked down SU/SR cells and challenged them with Chb-M'. As shown in Figure S6A-F, *p53* knockdown indeed conferred relative resistance to Chb-M' to a certain extent, suggesting a possible involvement of p53 in the Chb-M'-mediated tumor suppression in these cells, however, the growth of *p53*-silenced SU/SR cells was still effectively controlled by Chb-M' at submicromolar levels. Considering the significant resistance to Chb-M' conferred by *BCR-ABL1* overexpression in these cells (Figure 3E), these results overall indicated that the growth suppression mediated by Chb-M' was dependent on both functional p53 and *BCR-ABL1*, however possibly more on *BCR-ABL1* in these Ph$^+$ ALL cells.

3.4 | Chb-M' significantly suppresses the growth of Ph$^+$ ALL PDX cells by downregulating *BCR-ABL1* expression in vivo

We investigated the effects of Chb-M' on Ph$^+$ ALL PDX cells in vivo. We transplanted Ph$^+$ ALL PDX cells derived from the first relapse patient into NOG mice. At 2 wk after the transplantation, Chb-M'

administration was started to treat these mice. DMSO and imatinib mesylate were injected as controls (Figure 4A). Bone marrow was collected every week to check the chimerism of transplanted ALL cells. Chb-M' significantly suppressed the cell growth of Ph$^+$ ALL PDX cells in the bone marrow, compared with DMSO at week 5 (Figure 4B). NOG mice treated with Chb-M' had significantly prolonged overall survival compared with mice treated with DMSO (Figure 4C), which is consistent with the results observed in our previous in vivo experiments with the SU/SR Ph$^+$ ALL cell line.[21] The patient sample was negative for the T315I mutation, but imatinib did not prolong survival compared with controls in PDX experiments. To investigate the mechanism of imatinib resistance, we performed mutation analysis on the RNA-seq data of the PDX cells, and the results are listed in Table S4, which showed no mutations in the *ABL1* gene, including T315. The underlying mechanism of imatinib resistance in Ph$^+$ leukemia patients, in addition to mutations in the kinase domain of *ABL1*, has recently been shown to be due to the genomic amplification of *BCR-ABL1* or the upregulation of the *BCR-ABL1* transcript level.[33-35] FISH of *BCR-ABL1* showed that most leukemic cells at the patient's initial diagnosis had 3 signals of *BCR-ABL1*, indicating genomic amplification of *BCR-ABL1*. In addition, the mRNA expression of *RUNX1* and *BCR-ABL1* was increased in relapse-derived PDX cells compared with that in primary-derived PDX cells (Figure S7). This is consistent with the previous report that high expression of RUNX1 is associated with disease progression of CML.[18] From these results, the imatinib resistance in the PDX cells may be due to the increased expression of *BCR-ABL1* associated with increased copy number of *BCR-ABL1* and upregulation by RUNX1. As shown in the H&E staining and immunohistochemistry (human CD45 and Ki-67) panels, Chb-M' lessened the tumor burdens in the bone marrow relative to the controls. In addition, Chb-M' suppressed RUNX1 and BCR-ABL1 expression of leukemic cells as shown by immunohistochemistry (Figure 4D). Taken together, our RUNX inhibitor, Chb-M', could be used as a novel drug for patients with TKI-resistant refractory Ph$^+$ ALL through the downregulation of *BCR-ABL1* (Figure 4E).

4 | DISCUSSION

Runt-related transcription factor 1 (RUNX1) forms a heterodimeric complex with core binding factor-β (CBFβ) on DNA promoter regions and regulates the expression of diverse target genes that are essential for the survival of certain cancers. Yamamoto et al[18] have previously reported that functionally deregulated RUNX1 cooperates with BCR-ABL1 and induces a blastic phase-like phenotype of CML in mice. In this study, we found that RUNX1 directly targets *BCR-ABL1* in Ph$^+$ ALL cells through regulating the *BCR* promoter. According to Shah et al[36], a functional promoter of *BCR* is localized in a region 1000 bp upstream of the *BCR* exon 1 coding sequence, which includes the RUNX consensus binding sequence we identified in this study. In addition to this study, a few groups have previously studied and reported the functional regulation of the *BCR* promoter. For example, Sharma et al[37] have shown that
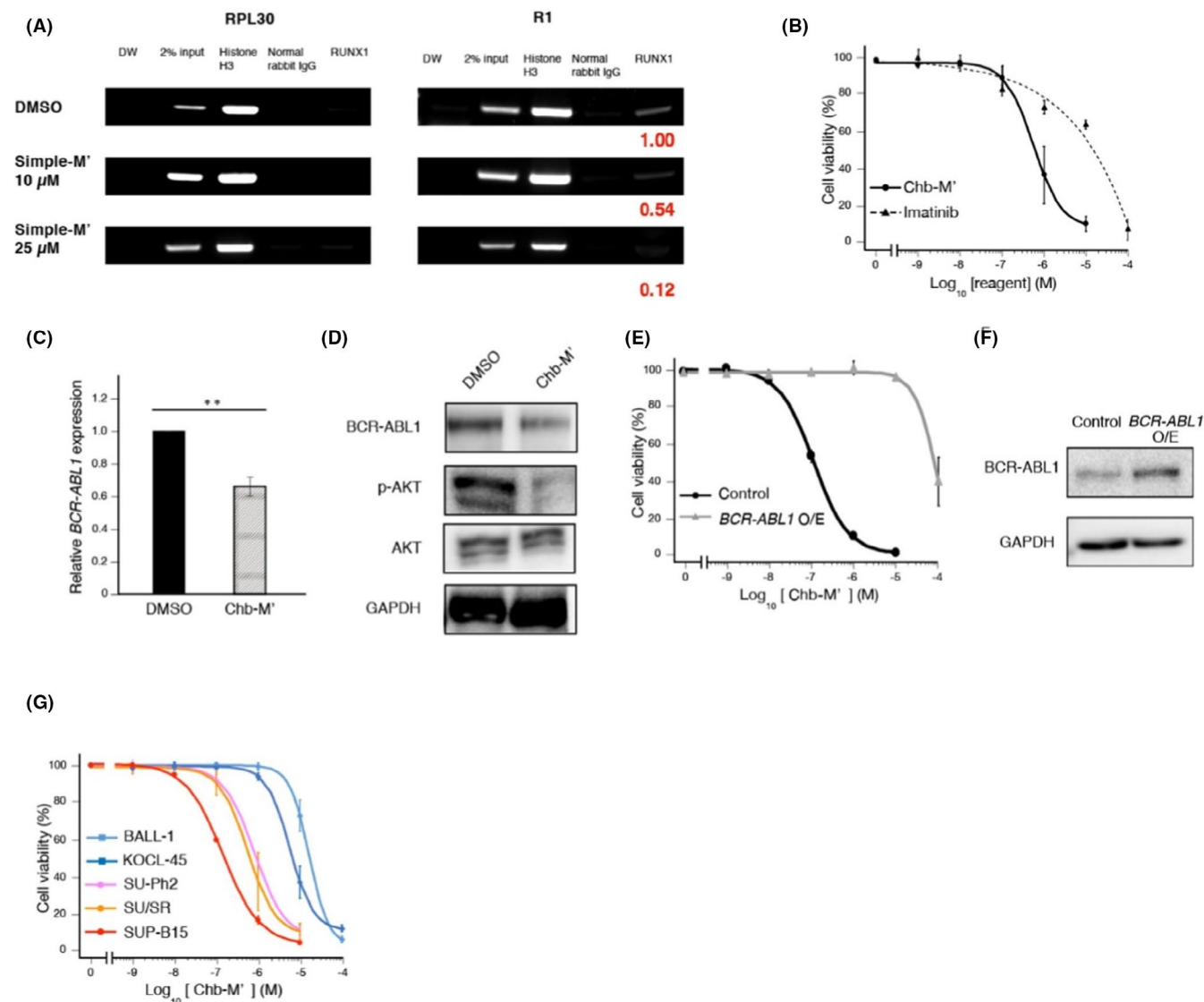
FIGURE 3 Anti-leukemic efficacy of RUNX inhibitor Chb-M' in Ph$^+$ ALL cells. A, Gel image of ChIP-PCR in SU/SR cells treated with DMSO or Simple-M' (10, 25 μmol L^{-1}) for 12 h in the same way as Figure 2E. Bands were quantified using Image Lab software (Bio-Rad Laboratories) and normalized to that of the control. B, Dose-response curves of SU/SR cells treated with the indicated doses of Chb-M' (IC50: 658 nmol L^{-1}) and imatinib (IC$_{50}$: 18.2 μmol L^{-1}) for 48 h. C, *BCR-ABL1* mRNA expression in SU/SR cells treated with DMSO or Chb-M' (1 μmol L^{-1}) for 9 h. D, Immunoblot of BCR-ABL1, phosphorylated-AKT (p-AKT), AKT and GAPDH in SU/SR cells treated with DMSO or Chb-M' (1 μmol L^{-1}) for 24 h. E, Dose-response curves of SU/SR cells stably transduced with control (IC$_{50}$: 143 nmol L^{-1}) or *BCR-ABL1* expressing vectors (IC50: 33.1 μmol L^{-1}) for 48 h. F, Immunoblot of BCR-ABL1 and GAPDH in (E). Cells were treated with 3 μmol L^{-1} doxycycline for 48 h. G, Dose-response curves of ALL cell lines with *BCR-ABL1* (SU-Ph2 [IC50: 849 nmol L^{-1}], SU/SR (IC$_{50}$: 658 nmol L^{-1}) and SUP-B15 [IC50: 167 nmol L^{-1}]) and ALL cell lines without *BCR-ABL1* (BALL-1 [IC50: 21.7 μmol L^{-1}] and KOCL-45 [IC50: 6.04 μmol L^{-1}]) treated with the indicated doses of Chb-M' for 48 h. Mean ±SD. **$P < .01$, using two-tailed Student *t* test (C)

MYC and MAX genes interact with the *BCR* promoter and regulate its transcription. To our knowledge, however, this is the first study that provides evidence for a possibility of pharmacological intervention in the transcriptional regulation of *BCR-ABL1* gene. As acquisition of point mutations in the *BCR-ABL1* gene is the major mechanism that hampers TKI-mediated tumor suppression in Ph$^+$ ALL patients, therapies that directly modulate the expression of *BCR-ABL1* can be a reasonable strategy to overcome the current clinical problems related to TKIs. Together with our previous finding that Chb-M' is highly effective against T315I mutation positive Ph$^+$

ALL cells even in vivo with minimal side effects,[21] our work not only unveiled the novel role of RUNX1 transcription factor in the trans-activation of *BCR-ABL1* expression, but also potentially provides alternative choice for the patients with TKI treatment-resistant Ph$^+$ ALL. Moreover, our study provides pieces of evidence that not only Ph$^+$ ALL cells but also CML cells might be efficiently controlled by RUNX1 inhibition.

Conversely, other RUNX inhibitors that stand on other mechanisms of action (ex. Ro5-3335[38]) should also be tested in these tumors to further validate our results. In addition, addressing the
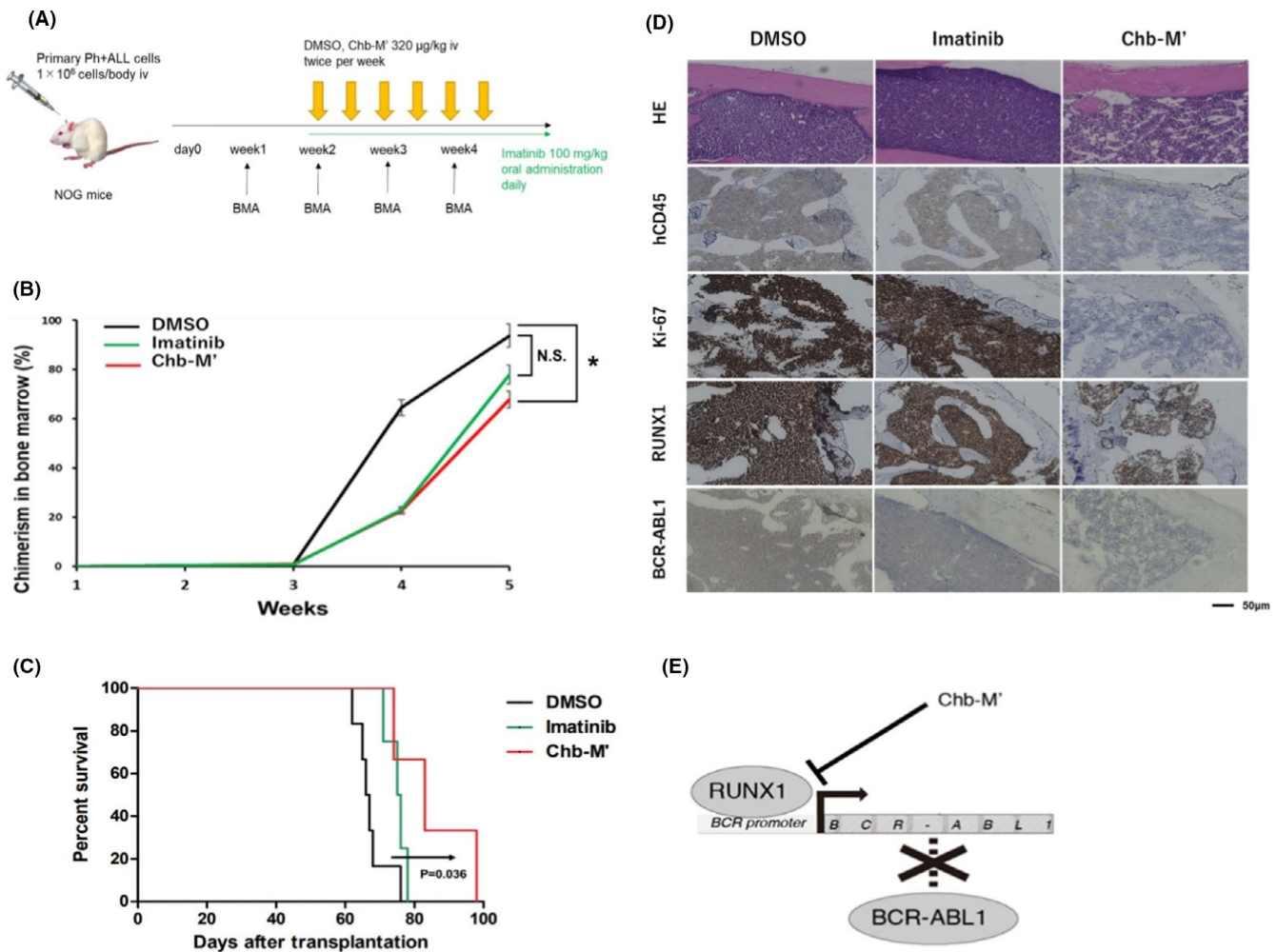
FIGURE 4 Chb-M' significantly suppresses the growth of Ph$^+$ ALL PDX cells by downregulating *BCR-ABL1* expression in vivo. A, Schema of transplantation assay in NOG mice with Ph$^+$ ALL PDX cells. These mice were treated with DMSO, imatinib mesylate or Chb-M'. B, Chimerism of transplanted leukemia cells in bone marrow (n = 7). C, Overall survival of NOG mice transplanted with Ph$^+$ ALL PDX cells (n = 6). D, Representative histology pictures of bone marrow at day 36. H&E staining and immunohistochemical staining with anti-human CD45 antibody, anti-Ki-67 antibody, anti-RUNX1 antibody and anti-BCR (BCR-ABL1) antibody were done for each slide (original magnification; ×10, Scale bars; 50 μm). E, Graphical abstract of this study. *RUNX1*-silencing inhibits the transactivation of *BCR-ABL1* expression and therefore attenuates the proliferation of *BCR-ABL1* fusion gene-dependent leukemia cells. Our RUNX inhibitor, Chb-M', could be potentially a novel drug for Ph$^+$ ALL with TKI resistance through the downregulation of *BCR-ABL1*. Mean ± SD. *P < .05, NS; not significant, using two-tailed Student t test (B), log-rank (C)

roles of other RUNX family members such as RUNX2 and RUNX3 will help elucidate how RUNX family transcription factors generally contribute to the pathogenesis of *BCR-ABL1* positive tumors including Ph$^+$ ALL. Although the role of BCR itself has not been fully elucidated in tumorigenesis, we are assuming that the RUNX inhibition strategy can potentially be applied to cancers that are dependent on BCR, such as metastatic colorectal cancer.[39] The efficacy of available RUNX inhibitors should also be tested in these tumors in future studies. From mutations of PDX cells (Table S4), based on known driver genes in pediatric B-cell precursor ALL,[40] we extracted the 2 driver genes, *MSH6* and *CREBBP*. Of them, *CREBBP* mutations have been identified as a mechanism of resistance in ALL,[41] and somatic variants in epigenetic modifiers including *CREBBP* can predict failure of response to imatinib in chronic-phase CML.[42] These suggest that

imatinib resistance in PDX cells may be due to the *CREBBP* mutation in addition to the high expression of *BCR-ABL1*.

In conclusion, we have discovered a vital role of the *RUNX1* transcription factor in the regulation of *BCR-ABL1* expression and in the maintenance of Ph$^+$ ALL cells not only in human leukemia cell lines but also in PDX cells. *RUNX1* could be an ideal target in the treatment of Ph$^+$ ALL, and future clinical trials with our novel RUNX inhibitor Chb-M' in these patients are awaited.

DISCLOSURE

The authors have no conflict of interest.

ORCID

Shintaro Maeda https://orcid.org/0000-0002-8932-2051
Itaru Kato https://orcid.org/0000-0002-2932-4960
Masahiro Hirata https://orcid.org/0000-0001-9211-0511
Yoichi Imai https://orcid.org/0000-0002-2938-6133
Shinya Kimura https://orcid.org/0000-0003-1717-6208
Yasuhiko Kamikubo https://orcid.org/0000-0003-2761-8508

REFERENCES

1. Malard F, Mohty M. Acute lymphoblastic leukaemia. *Lancet*. 2020;395(10230):1146-1162.
2. Pui CH, Yang JJ, Hunger SP, et al. Childhood acute lymphoblastic leukemia: progress through collaboration. *J Clin Oncol*. 2015;33(27):2938-2948.
3. Pui CH, Evans WE. Treatment of acute lymphoblastic leukemia. *N Engl J Med*. 2006;354(2):166-178.
4. Linabery AM, Ross JA. Trends in childhood cancer incidence in the U.S. (1992-2004). *Cancer*. 2008;112(2):416-432.
5. Smith MA, Seibel NL, Altekruse SF, et al. Outcomes for children and adolescents with cancer: challenges for the twenty-first century. *J Clin Oncol*. 2010;28(15):2625-2634.
6. Pui CH, Pei D, Campana D, et al. A revised definition for cure of childhood acute lymphoblastic leukemia. *Leukemia*. 2014;28(12):2336-2343.
7. Jabbour E, O'Brien S, Konopleva M, Kantarjian H. New insights into the pathophysiology and therapy of adult acute lymphoblastic leukemia. *Cancer*. 2015;121(15):2517-2528.
8. Sive JI, Buck G, Fielding A, et al. Outcomes in older adults with acute lymphoblastic leukaemia (ALL): results from the international MRC UKALL XII/ECOG2993 trial. *Br J Haematol*. 2012;157(4):463-471.
9. Ottmann OG, Pfeifer H. Management of Philadelphia chromosome-positive acute lymphoblastic leukemia (Ph+ ALL). *Hematology Am Soc Hematol Educ Program*. 2009;1:371-381.
10. Druker BJ, Sawyers CL, Kantarjian H, et al. Activity of a specific inhibitor of the BCR-ABL tyrosine kinase in the blast crisis of chronic myeloid leukemia and acute lymphoblastic leukemia with the Philadelphia chromosome [published correction appears in N Engl J Med 2001 Jul 19;345(3):232]. *N Engl J Med*. 2001;344(14):1038-1042.
11. Demetri GD, von Mehren M, Blanke CD, et al. Efficacy and safety of imatinib mesylate in advanced gastrointestinal stromal tumors. *N Engl J Med*. 2002;347(7):472-480.
12. Fielding AK, Rowe JM, Buck G, et al. UKALLXII/ECOG2993: addition of imatinib to a standard treatment regimen enhances long-term outcomes in Philadelphia positive acute lymphoblastic leukemia. *Blood*. 2014;123(6):843-850.
13. Soverini S, De Benedittis C, Papayannidis C, et al. Drug resistance and BCR-ABL kinase domain mutations in Philadelphia chromosome-positive acute lymphoblastic leukemia from the imatinib to the second-generation tyrosine kinase inhibitor era: the main changes are in the type of mutations, but not in the frequency of mutation involvement. *Cancer*. 2014;120(7):1002-1009.
14. Luciano L, Annunziata M, Attolico I, et al. The multi-tyrosine kinase inhibitor ponatinib for chronic myeloid leukemia: real-world data. *Eur J Haematol*. 2020;105(1):3-15.
15. Pavlovsky C, Chan O, Talati C, Pinilla-Ibarz J. Ponatinib in the treatment of chronic myeloid leukemia and Philadelphia chromosome positive acute lymphoblastic leukemia. *Future Oncol*. 2019;15(3):257-269.
16. Okuda T, van Deursen J, Hiebert SW, Grosveld G, Downing JR. AML1, the target of multiple chromosomal translocations in human leukemia, is essential for normal fetal liver hematopoiesis. *Cell*. 1996;84(2):321-330.
17. Hein D, Borkhardt A, Fischer U. Insights into the prenatal origin of childhood acute lymphoblastic leukemia. *Cancer Metastasis Rev*. 2020;39(1):161-171.
18. Yamamoto K, Tsuzuki S, Minami Y, et al. Functionally deregulated AML1/RUNX1 cooperates with BCR-ABL to induce a blastic phase-like phenotype of chronic myelogenous leukemia in mice. *PLoS One*. 2013;8(9):e74864. Published 2013 Sep 30.
19. Kamikubo Y, Zhao L, Wunderlich M, et al. Accelerated leukemogenesis by truncated CBF beta-SMMHC defective in high-affinity binding with RUNX1. *Cancer Cell*. 2010;17(5):455-468.
20. Hyde RK, Zhao L, Alemu L, Liu PP. Runx1 is required for hematopoietic defects and leukemogenesis in Cbfb-MYH11 knock-in mice. *Leukemia*. 2015;29(8):1771-1778.
21. Morita K, Suzuki K, Maeda S, et al. Genetic regulation of the RUNX transcription factor family has antitumor effects. *J Clin Invest*. 2017;127(7):2815-2828.
22. Morita K, Maeda S, Suzuki K, et al. Paradoxical enhancement of leukemogenesis in acute myeloid leukemia with moderately attenuated RUNX1 expressions. *Blood Adv*. 2017;1(18):1440-1451.
23. Morita K, Noura M, Tokushige C, et al. Autonomous feedback loop of RUNX1-p53-CBFB in acute myeloid leukemia cells. *Sci Rep*. 2017;7(1):16604.
24. Morita K, Tokushige C, Maeda S, et al. RUNX transcription factors potentially control E-selectin expression in the bone marrow vascular niche in mice. *Blood Adv*. 2018;2(5):509-515.
25. Chou TC, Talalay P. Quantitative analysis of dose-effect relationships: the combined effects of multiple drugs or enzyme inhibitors. *Adv Enzyme Regul*. 1984;22:27-55.
26. Morita K, Masamoto Y, Kataoka K, et al. BAALC potentiates oncogenic ERK pathway through interactions with MEKK1 and KLF4. *Leukemia*. 2015;29(11):2248-2256.
27. Weisberg E, Manley PW, Cowan-Jacob SW, Hochhaus A, Griffin JD. Second generation inhibitors of BCR-ABL for the treatment of imatinib-resistant chronic myeloid leukaemia. *Nat Rev Cancer*. 2007;7(5):345-356.
28. Hirase C, Maeda Y, Takai S, Kanamaru A. Hypersensitivity of Ph-positive lymphoid cell lines to rapamycin: possible clinical application of mTOR inhibitor. *Leuk Res*. 2009;33(3):450-459.
29. Redaelli S, Piazza R, Rostagno R, et al. Activity of bosutinib, dasatinib, and nilotinib against 18 imatinib-resistant BCR/ABL mutants. *J Clin Oncol*. 2009;27(3):469-471.
30. Müller MC, Cortes JE, Kim DW, et al. Dasatinib treatment of chronic-phase chronic myeloid leukemia: analysis of responses according to preexisting BCR-ABL mutations. *Blood*. 2009;114(24):4944-4953.
31. Bando T, Sugiyama H. Synthesis and biological properties of sequence-specific DNA-alkylating pyrrole-imidazole polyamides. *Acc Chem Res*. 2006;39(12):935-944.

32. Minoshima M, Bando T, Shinohara K, Sugiyama H. Molecular design of sequence specific DNA alkylating agents. *Nucleic Acids Symp Ser (Oxf)*. 2009;53:69-70.

33. Ossard-Receveur A, Bernheim A, Clausse B, et al. Duplication of the Ph-chromosome as a possible mechanism of resistance to imatinib mesylate in patients with chronic myelogenous leukemia. *Cancer Genet Cytogenet*. 2005;163(2):189-190.

34. Melo JV, Chuah C. Resistance to imatinib mesylate in chronic myeloid leukaemia. *Cancer Lett*. 2007;249(2):121-132.

35. Otero L, Ornellas MH, Dobbin J, de Souza FT. Double Philadelphia-chromosome: a resistance factor on the imatinib mesylate therapy for chronic myeloid leukemia. *Int J Lab Hematol*. 2008;30(4):346-348.

36. Shah NP, Witte ON, Denny CT. Characterization of the BCR promoter in Philadelphia chromosome-positive and -negative cell lines. *Mol Cell Biol*. 1991;11(4):1854-1860.

37. Sharma N, Magistroni V, Piazza R, et al. BCR/ABL1 and BCR are under the transcriptional control of the MYC oncogene. *Mol Cancer*. 2015;14:132. Published 2015 Jul 16.

38. Cunningham L, Finckbeiner S, Hyde RK, et al. Identification of benzodiazepine Ro5-3335 as an inhibitor of CBF leukemia through quantitative high throughput screen against RUNX1-CBFβ interaction. *Proc Natl Acad Sci USA*. 2012;109(36):14592-14597.

39. Jeitany M, Leroy C, Tosti P, et al. Inhibition of DDR1-BCR signalling by nilotinib as a new therapeutic strategy for metastatic colorectal cancer. *EMBO Mol Med*. 2018;10(4):e7918.

40. Ueno H, Yoshida K, Shiozawa Y, et al. Landscape of driver mutations and their clinical impacts in pediatric B-cell precursor acute lymphoblastic leukemia. *Blood Adv*. 2020;4(20):5165-5173.

41. Mullighan CG, Zhang J, Kasper LH, et al. CREBBP mutations in relapsed acute lymphoblastic leukaemia. *Nature*. 2011;471(7337):235-239.

42. Nteliopoulos G, Bazeos A, Claudiani S, et al. Somatic variants in epigenetic modifiers can predict failure of response to imatinib but not to second-generation tyrosine kinase inhibitors. *Haematologica*. 2019;104(12):2400-2409.

SUPPORTING INFORMATION

Additional supporting information may be found in the online version of the article at the publisher's website.
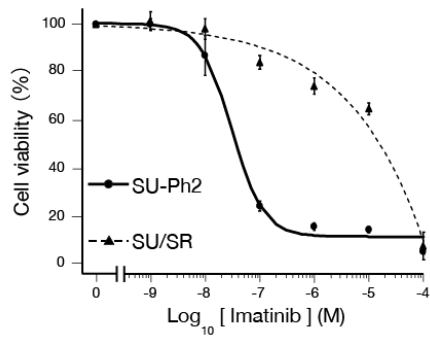
Figure S1

Dose-response curves of SU-Ph2 (IC50 value: 38.2 nM) and SU/SR (IC50 value: 18.2 μM) cells treated with the indicated doses of imatinib for 48 hours (Three independent experiments). Mean ± SD.

Figure S2
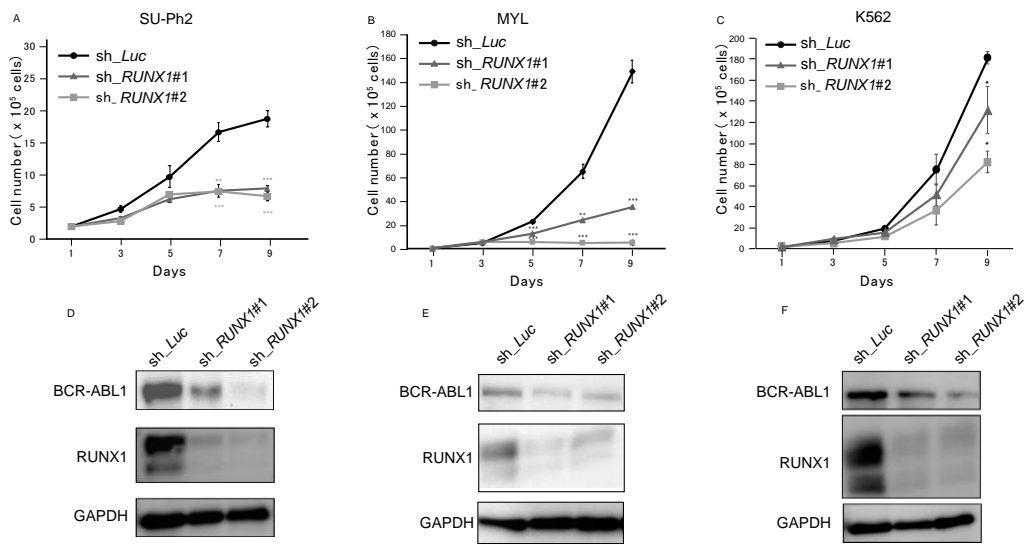
(A-C) Cell growth curves of SU-Ph2 (A), MYL (B) and K562 (C) cells transduced with sh_*Luc*. or sh_*RUNX1*. Mean $\pm$ SD (Three independent experiments). *P < 0.05, **P < 0.01, ***P < 0.001.

(D-F) Immunoblot of BCR-ABL1, RUNX1 and GAPDH in SU-Ph2 (D), MYL (E) and K562 (F) cells transduced with sh_*Luc* or sh_*RUNX1*. Cells were cultured with 3 μM doxycycline for 48 hours before lysed for protein extraction.

Figure S3

A

B
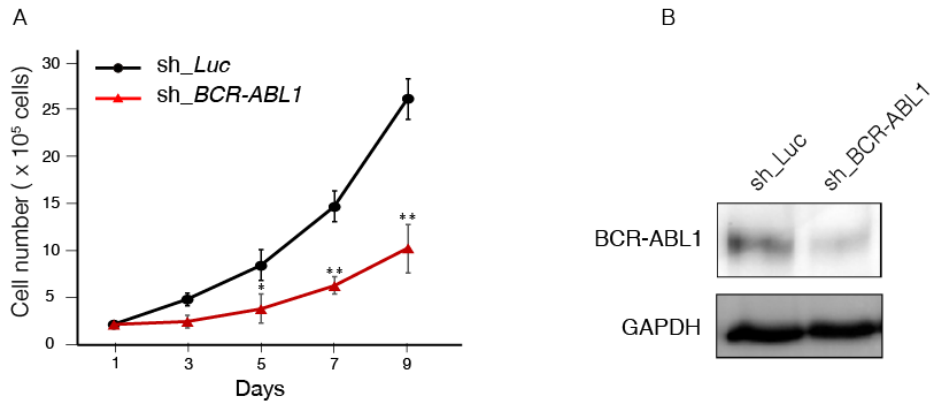
(A) Cell growth curves of SU/SR cells transduced with sh_*Luc* or sh_*BCR-ABL1*. Mean ± SD (Three independent experiments). * P < 0.05, ** P < 0.01.

(B) Immunoblot of BCR-ABL1 and GAPDH in SU/SR cells transduced with sh_*Luc* or sh_*BCR-ABL1*. Cells were cultured with 3 μM doxycycline for 48 hours before lysed for protein extraction.

Figure S4
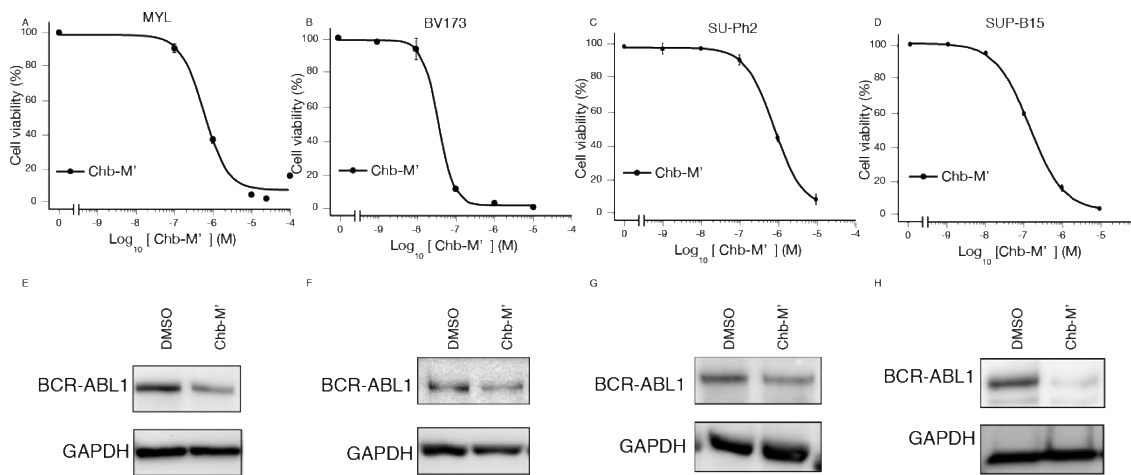
(A-D) Dose-response curves of CML and Ph+ ALL cells treated with the indicated doses of Chb-M' for 48 hours. MYL (A, IC value: 575 nM) and BV173 (B, IC value: 33 nM) cells are derived from CML cells, and SU-Ph2 (C, IC value: 849 nM) and SUP-B15 (D, IC value: 153 nM) cells are derived from Ph+ ALL cells (Three independent experiments). Values are mean ± SD.

(E-H) Immunoblot of BCR-ABL1 and GAPDH in MYL (E), BV173 (F), SU-Ph2 (G) and SUP-B15 (H) cells treated with Chb-M' or control DMSO for 24 hours.

Figure S5
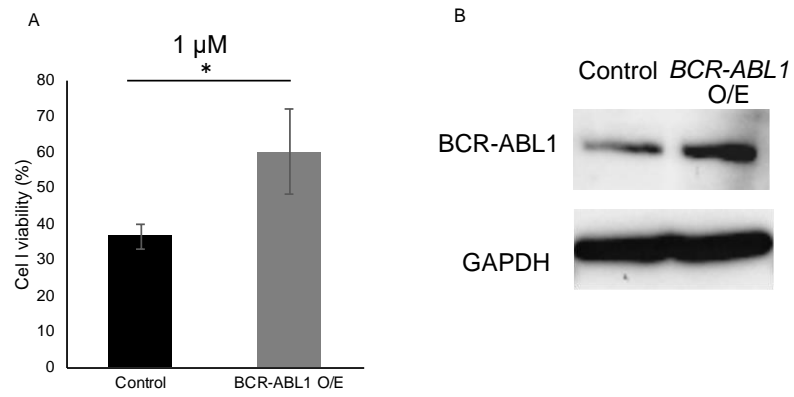
(A) Cell viability (% of untreated) of control and *BCR-ABL1* O/E MYL treated with Chb-M' 1 µM for 48 hours. Mean ± SD (Three independent experiments), * P < 0.05.

(B) Immunoblot of BCR-ABL1 and GAPDH in MYL.

Figure S6
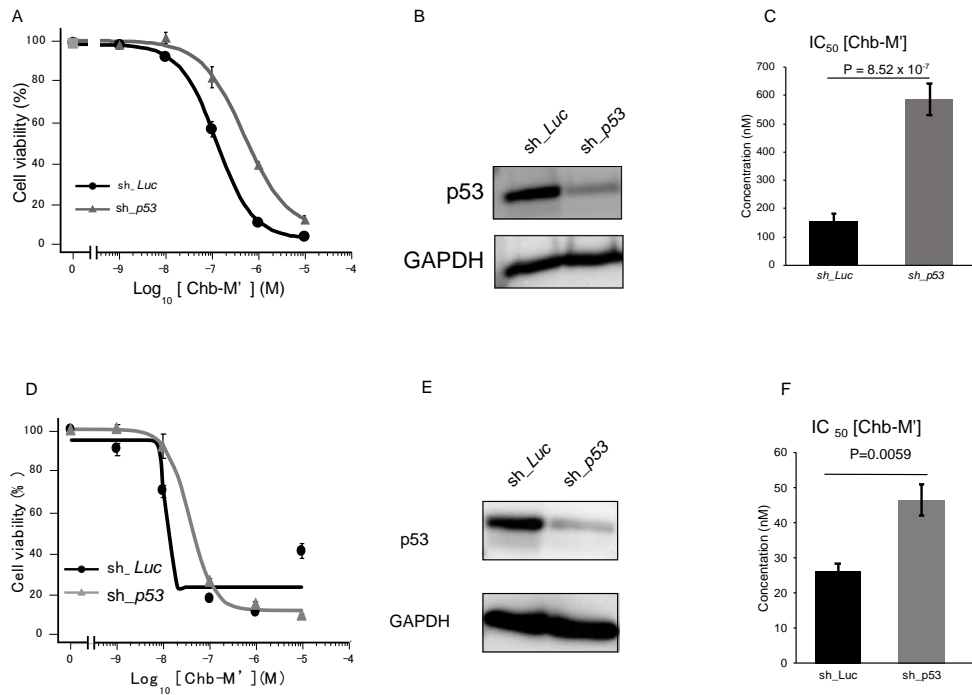
(A) Dose-response curves of SU/SR cells transduced with sh_*Luc* or sh_*p53* treated with the indicated doses of Chb-M' for 48 hours (n =4). Values are mean ± SD.

(B) Immunoblot of p53 and GAPDH in SU/SR cells transduced with sh_*Luc* or sh_*p53*. Cells were cultured with 3 μM doxycycline for 48 hours before lysed for protein extraction.

(C) IC$_{50}$ values of Chb-M' for 48 hours in SU/SR cells transduced with sh_*Luc* or sh_*p53*. Values are mean ± SD (n = 4).

(D) Dose-response curves of BV173 cells transduced with sh_*Luc* or sh_*p53* treated with the indicated doses of Chb-M' for 48 hours (n =3). Values are mean ± SD.

(E) Immunoblot of p53 and GAPDH in BV173 cells transduced with sh_*Luc* or sh_*p53*. Cells were cultured with 3 μM doxycycline for 24 hours before lysed for protein extraction.

(F) IC$_{50}$ values of Chb-M' for 48 hours in BV173 cells transduced with sh_*Luc* or sh_*p53*. Values are mean ± SD (n = 3).

Figure S7
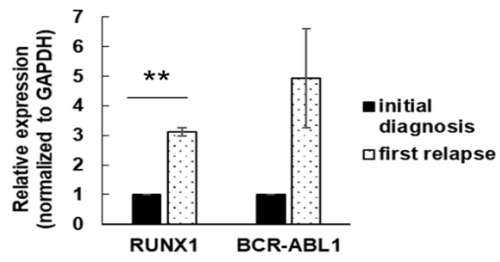
Relative expressions of *RUNX1* and *BCR-ABL1* in PDX cells at two timings (initial diagnosis or first relapse). Cells were processed for RT-qPCR. Values were normalized to that of initial diagnosis (Three independent experiments). Mean ± SEM, **$P < 0.01$.

Table S1

PCR primers used for RT -qPCR

	Forward (5' → 3')	Reverse (5' → 3')
GAPDH	CATGTTCGTCATGGGGTGAACCA	AGTGATGGCATGGACTGTGGTCAT
RUNX1	CTGCTCCGTGCTGCCTAC	AGCCATCACAGTGACCAGAGT
BCR-ABL1	AACTCGCAACAGTCCTTCGAC	CCATTCCCCATTGTGATTATAGC

able S2

PCR primers used for ChIP

	Forward (5' → 3')	Reverse (5' → 3')
BCR-ABL1 promoter R1	AGGCAGGTGTGGGTATTGAG	CCAGGCTGAGTAACCAATGC

Table S3

Target sequences for shRNA knockdown experiments

	Targets
sh_*RUNX1* #1	AGCTTCACTCTGACCATCA
sh_*RUNX1* #2	AACCTCGAAGACATCGGCA
sh_ *Luc*	CGTACGCGGAATACTTCGA
sh_*BCR-ABL1*	GGGTCTTAGGCTATAATCA
sh_*p53*	ACCATCCACTACAACTACA

Table S4

List of mutations identified by mutation analysis from RNA-seq

Chr	Start	End	Ref	Alt	Func.refGene	Gene.refGene	GeneDetail.refGene	ExonicFunc.refGene	AAChange.refGene
1	1271754	1271754	C	T	exonic	DVL1	.	nonsynonymous SNV	DVL1:NM_001330311:exon15:c.G1856A:p.R
1	2340068	2340068	C	G	exonic	PEX10	.	synonymous SNV	PEX10:NM_002617:exon3:c.G423C:p.A141A
1	22816843	22816843	A	T	exonic	ZBTB40	.	synonymous SNV	ZBTB40:NM_001330398:exon2:c.A402T:p.S
1	89448729	89448729	C	T	exonic	RBMXL1	.	nonsynonymous SNV	RBMXL1:NM_019610:exon2:c.G781A:p.G26
1	89448733	89448733	G	T	exonic	RBMXL1	.	synonymous SNV	RBMXL1:NM_019610:exon2:c.C777A:p.G25
1	100376372	100376372	G	C	exonic	AGL	.	nonsynonymous SNV	AGL:NM_000028:exon28:c.G3805C:p.A1269
1	145299787	145299787	T	G	exonic	NBPF10	.	nonsynonymous SNV	NBPF10:NM_001039703:exon6:c.T836G:p.L
1	145299906	145299906	T	G	exonic	NBPF10	.	nonsynonymous SNV	NBPF10:NM_001039703:exon6:c.T955G:p.S
1	148252049	148252049	A	C	exonic	NBPF14	.	synonymous SNV	NBPF14:NM_015383:exon66:c.T8286G:p.S2
1	149783759	149783759	A	T	exonic	HIST2H2BF	.	synonymous SNV	HIST2H2BF:NM_001024599:exon1:c.T120A
1	158990320	158990320	G	A	splicing	IFI16	NM_0013648 6	.	.
1	161495096	161495096	T	C	exonic	HSPA6	.	synonymous SNV	HSPA6:NM_002155:exon1:c.T648C:p.A216A
1	161495275	161495275	T	C	exonic	HSPA6	.	nonsynonymous SNV	HSPA6:NM_002155:exon1:c.T827C:p.L276P
1	161495338	161495338	C	A	exonic	HSPA6	.	nonsynonymous SNV	HSPA6:NM_002155:exon1:c.C890A:p.T297K
2	15737558	15737558	-	A	exonic	DDX1	.	frameshift insertion	DDX1:NM_004939:exon5:c.223dupA:p.G77f
2	16745267	16745267	G	A	exonic	FAM49A	.	synonymous SNV	FAM49A:NM_030797:exon5:c.C288T:p.S96S
2	32641033	32641033	-	A	exonic	BIRC6	.	frameshift insertion	BIRC6:NM_016252:exon10:c.2675dupA:p.T5
2	44153096	44153096	G	T	exonic	LRPPRC	.	nonsynonymous SNV	LRPPRC:NM_133259:exon26:c.C2741A:p.P9
2	48033499	48033499	T	C	splicing	MSH6	NM_000179:ex	.	.
2	67624714	67624714	C	T	exonic	ETAA1	.	nonsynonymous SNV	ETAA1:NM_019002:exon1:c.C134T:p.P45L
2	73478562	73478562	T	G	splicing	CCT7	NM_0011662 8	.	.
2	174231876	174231876	A	C	splicing	CDCA7	NM_031942:ex	.	.
2	178988570	178988570	G	A	exonic	RBM45	.	nonsynonymous SNV	RBM45:NM_001365578:exon7:c.G999A:p.M
2	201756797	201756797	C	T	exonic	NIF3L1	.	nonsynonymous SNV	NIF3L1:NM_001142356:exon1:c.C131T:p.S4
2	203162237	203162237	G	A	splicing	NOP58	NM_015934:ex	.	.
2	206911262	206911262	A	G	exonic	INO80D	.	nonsynonymous SNV	INO80D:NM_017759:exon5:c.T1039C:p.S34
2	242618032	242618032	G	T	exonic	DTYMK	.	nonsynonymous SNV	DTYMK:NM_001320902:exon3:c.C234A:p.D
3	14444330	14444330	-	A	splicing	SLC6A6	NM_0011436 7	.	.
3	40208373	40208373	G	A	exonic	MYRIP	.	nonsynonymous SNV	MYRIP:NM_001284426:exon4:c.G26A:p.R9C
3	122422624	122422624	C	T	exonic	PARP14	.	synonymous SNV	PARP14:NM_017554:exon7:c.C3117T:p.L10
3	132432080	132432080	-	A	exonic	NPHP3	.	frameshift insertion	NPHP3:NM_153240:exon6:c.1007dupT:p.H3
3	146233866	146233866	G	T	exonic	PLSCR1	.	nonsynonymous SNV	PLSCR1:NM_021105:exon7:c.680A:p.T
3	160156629	160156629	-	T	exonic	TRIM59	.	frameshift insertion	TRIM59:NM_173084:exon3:c.342dupA:p.L1
3	169700647	169700647	-	A	exonic	SEC62	.	frameshift insertion	SEC62:NM_003262:exon4:c.405dupA:p.E13
3	179320465	179320465	-	T	exonic	MRPL47	.	frameshift insertion	MRPL47:NM_020409:exon2:c.218dupA:p.N7
3	188327369	188327369	G	C	exonic	LPP	.	nonsynonymous SNV	LPP:NM_001167671:exon6:c.G850C:p.E284
3	196199614	196199614	-	A	exonic	RNF168	.	frameshift insertion	RNF168:NM_152317:exon6:c.791_792insT:p
3	196630421	196630421	-	T	exonic	SENP5	.	frameshift insertion	SENP5:NM_001308045:exon6:c.1825dupT:p
4	435649	435649	T	G	exonic	ZNF721	.	nonsynonymous SNV	ZNF721:NM_133474:exon3:c.A2607C:p.E86
4	437056	437056	A	C	exonic	ZNF721	.	nonsynonymous SNV	ZNF721:NM_133474:exon3:c.T1200G:p.S40
4	2940026	2940026	T	C	exonic	NOP14	.	nonsynonymous SNV	NOP14:NM_001291979:exon17:c.A2335G:p
4	3318650	3318650	C	T	exonic	RGS12	.	synonymous SNV	RGS12:NM_002926:exon2:c.C753T:p.S251S
4	8288480	8288480	G	A	exonic	HTRA3	.	synonymous SNV	HTRA3:NM_001297559:exon3:c.G678A:p.S2
4	68383962	68383962	G	T	exonic	CENPC	.	synonymous SNV	CENPC:NM_001363481:exon7:c.C742A:p.R:
4	73968215	73968215	-	T	exonic	ANKRD17	.	frameshift insertion	ANKRD17:NM_198889:exon24:c.3697dupA:
4	156631708	156631708	G	A	exonic	GUCY1A1	.	nonsynonymous SNV	GUCY1A1:NM_001130684:exon5:c.G391A:p
5	179994113	179994113	-	T	exonic	CNOT6	.	frameshift insertion	CNOT6:NM_001370474:exon7:c.459dupT:p
6	27925818	27925818	C	T	exonic	OR2B6	.	nonsynonymous SNV	OR2B6:NM_012367:exon1:c.C800T:p.S267F
6	33284498	33284498	G	A	exonic	ZBTB22	.	nonsynonymous SNV	ZBTB22:NM_001145338:exon2:c.C196T:p.F
6	33287891	33287891	T	C	exonic	DAXX	.	synonymous SNV	DAXX:NM_001254717:exon4:c.A1137G:p.E3
6	49403330	49403330	G	A	exonic	MMUT	.	nonsynonymous SNV	MMUT:NM_000255:exon12:c.C1963T:p.R65
6	79680524	79680524	-	T	exonic	PHIP	.	frameshift insertion	PHIP:NM_017934:exon25:c.2970dupA:p.Q9
6	84862599	84862599	-	T	exonic	CEP162	.	frameshift insertion	CEP162:NM_001286206:exon23:c.3065dupA
6	108385419	108385419	-	A	exonic	OSTM1	.	stopgain	OSTM1:NM_014028:exon2:c.486dupT:p.N1(
6	116967057	116967057	-	T	exonic	ZUP1	.	frameshift insertion	ZUP1:NM_001361191:exon8:c.920dupA:p.N
7	2583400	2583400	C	T	exonic	BRAT1	.	synonymous SNV	BRAT1:NM_001350627:exon4:c.G102A:p.A3
7	4841381	4841381	C	T	exonic	RADIL	.	synonymous SNV	RADIL:NM_018059:exon12:c.G2745A:p.G91
7	7645613	7645613	-	A	exonic	MIOS	.	frameshift insertion	MIOS:NM_001370078:exon8:c.2131dupA:p.
7	11075334	11075334	-	A	exonic	PHF14	.	frameshift insertion	PHF14:NM_001007157:exon8:c.1524dupA:p
7	39990548	39990548	A	G	exonic	CDK13	.	nonsynonymous SNV	CDK13:NM_003718:exon1:c.A308G:p.Q103I
7	74193642	74193642	G	A	exonic	NCF1	.	nonsynonymous SNV	NCF1:NM_000265:exon4:c.G269A:p.R90H
7	92764168	92764168	G	A	exonic	SAMD9L	.	synonymous SNV	SAMD9L:NM_001303500:exon4:c.C1117T:p
7	99129067	99129067	C	A	exonic	ZKSCAN5	.	nonsynonymous SNV	ZKSCAN5:NM_001318083:exon5:c.C1496A
7	105254688	105254688	A	T	exonic	ATXN7L1	.	nonsynonymous SNV	ATXN7L1:NM_138495:exon8:c.T1721A:p.L5
7	130351748	130351748	G	A	exonic	COPG2	.	nonsynonymous SNV	COPG2:NM_001290033:exon3:c.C112T:p.P3
8	90993682	90993682	C	T	exonic	NBN	.	nonsynonymous SNV	NBN:NM_002485:exon3:c.G241A:p.E81K
8	141460909	141460909	-	TGAG	exonic	TRAPPC9	.	frameshift insertion	TRAPPC9:NM_001160372:exon2:c.563_564
8	145010117	145010117	G	-	exonic	PLEC	.	nonsynonymous SNV	PLEC:NM_201378:exon6:c.G459C:p.W153C
8	145624592	145624592	-	CCGCAG	exonic	CPSF1	.	nonframeshift insertion	CPSF1:NM_013291:exon15:c.1392_1393ins
9	405014	405014	-	TT	exonic	DOCK8	.	frameshift insertion	DOCK8:NM_001190458:exon25:c.3031_303
9	19378704	19378704	A	T	splicing	RPS6	NM_001010:ex	.	.
9	131196787	131196787	A	C	exonic	CERCAM	.	nonsynonymous SNV	CERCAM:NM_001286760:exon11:c.A1196C
10	5691034	5691034	A	C	exonic	ASB13	.	nonsynonymous SNV	ASB13:NM_024701:exon4:c.T416G:p.V139C
10	60148569	60148569	-	AA	exonic	TFAM	.	frameshift insertion	TFAM:NM_001270782:exon4:c.431_432ins/
10	105883864	105883864	C	G	exonic	SFR1	.	synonymous SNV	SFR1:NM_001002759:exon3:c.C528G:p.V17
10	126454015	126454015	-	A	exonic	EEF1AKMT2	.	frameshift insertion	EEF1AKMT2:NM_001304467:exon5:c.327d
10	134038000	134038000	C	T	exonic	STK32C	.	nonsynonymous SNV	STK32C:NM_001318878:exon8:c.G943A:p.A
11	8016065	8016065	G	T	splicing	EIF3F	NM_003754:ex	.	.
11	18105213	18105213	-	T	exonic	SAAL1	.	frameshift insertion	SAAL1:NM_138421:exon10:c.1107dupA:p.P
11	34101202	34101202	G	A	exonic	CAPRIN1	.	nonsynonymous SNV	CAPRIN1:NM_005898:exon7:c.G716A:p.R23
11	57327825	57327825	G	A	exonic	UBE2L6	.	synonymous SNV	UBE2L6:NM_004223:exon2:c.C108T:p.H36I
11	62327540	62327540	C	G	splicing	EEF1G	NM_001404:ex	.	.
11	65733992	65733992	C	T	exonic	SART1	.	nonsynonymous SNV	SART1:NM_005146:exon9:c.C1153T:p.R385
11	66393989	66393989	G	A	exonic	RBM14	.	synonymous SNV	RBM14:NM_006328:exon3:c.G1860A:p.S62(
11	67021747	67021747	G	A	exonic	KDM2A	.	synonymous SNV	KDM2A:NM_001256405:exon9:c.G1848A:p.
11	67068486	67068486	G	A	exonic	ANKRD13D	.	nonsynonymous SNV	ANKRD13D:NM_207354:exon11:c.G1099A:p
11	75113393	75113393	A	G	exonic	RPS3	.	nonsynonymous SNV	RPS3:NM_001260506:exon4:c.A301G:p.K10
11	104905165	104905165	C	T	exonic	CASP1	.	nonsynonymous SNV	CASP1:NM_001223:exon2:c.G44A:p.R15H,C

12	6645958	6645958	T	C	splicing	GAPDH	NM_00128974(	.		.
12	6711174	6711174	G	T	exonic	CHD4	.		synonymous SNV	CHD4:NM_001297553:exon3:c.C369A:p.S1
12	6883957	6883957	T	C	exonic	LAG3	.		synonymous SNV	LAG3:NM_002286:exon4:c.T708C:p.S236S
12	6973884	6973884	A	C	splicing	USP5	NM_003481:ex	.		.
12	7171657	7171657	C	T	exonic	C1S	.		nonsynonymous SNV	C1S:NM_001734:exon5:c.C478T:p.P160S,C
12	12788823	12788823	-	A	exonic	CREBL2	.		frameshift insertion	CREBL2:NM_001310:exon2:c.129dupA:p.L4
12	31242081	31242081	G	A	exonic	DDX11	.		nonsynonymous SNV	DDX11:NM_001257144:exon7:c.G788A:p.R:
12	31255383	31255383	A	C	exonic	DDX11	.		nonsynonymous SNV	DDX11:NM_004399:exon22:c.A2144C:p.Q7:
12	120151400	120151400	-	ACCT	exonic	CIT	.		frameshift insertion	CIT:NM_007174:exon33:c.4233_4234insAG(
12	132445399	132445399	G	A	exonic	EP400	.		nonsynonymous SNV	EP400:NM_015409:exon2:c.G235A:p.V79M
13	25670907	25670907	C	A	exonic	PABPC3	.		nonsynonymous SNV	PABPC3:NM_030979:exon1:c.C571A:p.P19:
13	25671092	25671092	T	C	exonic	PABPC3	.		synonymous SNV	PABPC3:NM_030979:exon1:c.T756C:p.N25:
13	25671122	25671122	C	T	exonic	PABPC3	.		synonymous SNV	PABPC3:NM_030979:exon1:c.C786T:p.Y26:
13	25671172	25671172	C	A	exonic	PABPC3	.		nonsynonymous SNV	PABPC3:NM_030979:exon1:c.C836A:p.T27!
13	25671188	25671188	G	A	exonic	PABPC3	.		synonymous SNV	PABPC3:NM_030979:exon1:c.G852A:p.K28
13	25671320	25671320	A	G	exonic	PABPC3	.		synonymous SNV	PABPC3:NM_030979:exon1:c.A984G:p.E32
13	25671465	25671465	T	C	exonic	PABPC3	.		nonsynonymous SNV	PABPC3:NM_030979:exon1:c.T1129C:p.Y3
13	25671477	25671477	G	C	exonic	PABPC3	.		nonsynonymous SNV	PABPC3:NM_030979:exon1:c.G1141C:p.E3
13	25672058	25672058	G	T	exonic	PABPC3	.		synonymous SNV	PABPC3:NM_030979:exon1:c.G1722T:p.G5
13	25672211	25672211	T	C	exonic	PABPC3	.		synonymous SNV	PABPC3:NM_030979:exon1:c.T1875C:p.A6:
13	27690693	27690693	T	C	exonic	USP12	.		nonsynonymous SNV	USP12:NM_182488:exon2:c.A89G:p.E30G
13	46090370	46090370	A	G	exonic	COG3	.		synonymous SNV	COG3:NM_031431:exon17:c.A1902G:p.E63
13	46090371	46090371	A	G	exonic	COG3	.		nonsynonymous SNV	COG3:NM_031431:exon17:c.A1903G:p.I635
13	53217140	53217140	G	T	exonic	HNRNPA1L2	.		nonsynonymous SNV	HNRNPA1L2:NM_001011725:exon6:c.G513
13	53217171	53217171	C	T	exonic	HNRNPA1L2	.		nonsynonymous SNV	HNRNPA1L2:NM_001011725:exon6:c.C544
13	53217419	53217419	C	G	exonic	HNRNPA1L2	.		synonymous SNV	HNRNPA1L2:NM_001011725:exon6:c.C792
13	53217526	53217526	A	G	exonic	HNRNPA1L2	.		nonsynonymous SNV	HNRNPA1L2:NM_001011725:exon6:c.A899
13	53217547	53217547	T	G	exonic	HNRNPA1L2	.		nonsynonymous SNV	HNRNPA1L2:NM_001011725:exon6:c.T920(
14	24614675	24614675	C	T	splicing	PSME2	NM_002818:ex	.		.
14	39648566	39648566	A	C	exonic	PNN	.		nonsynonymous SNV	PNN:NM_002687:exon8:c.A693C:p.K231N
14	81670282	81670282	G	T	exonic	GTF2A1	.		nonsynonymous SNV	GTF2A1:NM_015859:exon3:c.C299A:p.A10(
14	96779721	96779721	G	T	exonic	ATG2B	.		nonsynonymous SNV	ATG2B:NM_018036:exon24:c.C3694A:p.P1:
14	102467991	102467991	G	A	exonic	DYNC1H1	.		synonymous SNV	DYNC1H1:NM_001376:exon21:c.G4515A:p.
14	102550129	102550129	C	G	splicing	HSP90AA1	NM_005348:ex	.		.
15	28447283	28447283	G	A	exonic	HERC2	.		synonymous SNV	HERC2:NM_004667:exon47:c.C7593T:p.D2!
15	34675050	34675050	C	T	exonic	GOLGA8A	.		nonsynonymous SNV	GOLGA8A:NM_181077:exon11:c.G1055A:p.I
15	34821271	34821271	C	T	exonic	GOLGA8B	.		nonsynonymous SNV	GOLGA8B:NM_001023567:exon11:c.G1055/
15	52620057	52620057	-	T	exonic	MYO5A	.		frameshift insertion	MYO5A:NM_001142495:exon34:c.4545dupA
15	64689965	64689965	G	A	exonic	TRIP4	.		nonsynonymous SNV	TRIP4:NM_016213:exon4:c.G566A:p.R189H
15	72640077	72640077	A	G	exonic	HEXA	.		nonsynonymous SNV	HEXA:NM_000520:exon10:c.T1096C:p.Y366
15	75652043	75652043	C	G	exonic	MAN2C1	.		nonsynonymous SNV	MAN2C1:NM_001256496:exon14:c.G1569C
15	85341891	85341891	C	T	exonic	ZNF592	.		nonsynonymous SNV	ZNF592:NM_014630:exon8:c.C2809T:p.R9:
15	101561294	101561294	C	T	exonic	LRRK1	.		nonsynonymous SNV	LRRK1:NM_024652:exon13:c.C1646T:p.S54
16	705658	705658	C	T	exonic	WDR90	.		nonsynonymous SNV	WDR90:NM_145294:exon16:c.C1804T:p.R6(
16	1555455	1555455	C	T	exonic	TELO2	.		synonymous SNV	TELO2:NM_001351846:exon16:c.C1887T:p.
16	3807936	3807936	G	T	exonic	CREBBP	.		nonsynonymous SNV	CREBBP:NM_001079846:exon17:c.C3369A:
16	4924667	4924667	-	A	exonic	UBN1	.		frameshift insertion	UBN1:NM_001079514:exon15:c.2257dupA:
16	16235066	16235066	C	T	exonic	ABCC1	.		synonymous SNV	ABCC1:NM_004996:exon31:c.C4524T:p.Y1!
16	18902199	18902199	G	A	exonic	SMG1	.		synonymous SNV	SMG1:NM_015092:exon5:c.C594T:p.D198D
16	29401304	29401304	C	T	exonic	NPIPB11	.		nonsynonymous SNV	NPIPB11:NM_001301304:exon5:c.G503A:p.
16	58550559	58550559	C	T	exonic	SETD6	.		synonymous SNV	SETD6:NM_001160305:exon4:c.C654T:p.A:
16	67964838	67964838	G	A	exonic	CTRL	.		nonsynonymous SNV	CTRL:NM_001907:exon3:c.C221T:p.A74V
16	86612832	86612832	C	T	exonic	FOXL1	.		nonsynonymous SNV	FOXL1:NM_005250:exon1:c.C503T:p.A168V
16	89762056	89762056	G	A	exonic	CDK10	.		nonsynonymous SNV	CDK10:NM_001098533:exon13:c.G808A:p./
17	4635097	4635097	-	A	exonic	MED11	.		frameshift insertion	MED11:NM_001001683:exon2:c.113dupA:p:
17	10101630	10101630	G	A	exonic	GAS7	.		synonymous SNV	GAS7:NM_201433:exon1:c.C78T:p.G26G
17	38975287	38975287	T	C	exonic	KRT10	.		synonymous SNV	KRT10:NM_000421:exon7:c.A1500G:p.G50(
17	43552478	43552478	C	T	exonic	PLEKHM1	.		nonsynonymous SNV	PLEKHM1:NM_001352825:exon4:c.G911A:p
17	46154354	46154354	-	T	exonic	CBX1	.		frameshift insertion	CBX1:NM_001127228:exon2:c.12dupA:p.Q5
17	57656854	57656854	C	T	exonic	DHX40	.		synonymous SNV	DHX40:NM_001166301:exon8:c.C864T:p.F2:
17	65688935	65688935	-	A	exonic	PITPNC1	.		frameshift insertion	PITPNC1:NM_012417:exon9:c.931dupA:p.A
17	65850790	65850790	-	A	exonic	BPTF	.		frameshift insertion	BPTF:NM_004459:exon2:c.1349dupA:p.N4!
17	74013889	74013889	G	A	exonic	EVPL	.		synonymous SNV	EVPL:NM_001320747:exon14:c.C1707T:p.A
18	32833578	32833578	A	G	exonic	ZSCAN30	.		nonsynonymous SNV	ZSCAN30:NM_001288711:exon2:c.T760C:p
18	60639893	60639893	-	A	exonic	PHLPP1	.		frameshift insertion	PHLPP1:NM_194449:exon15:c.3708dupA:p.
18	71959097	71959097	C	G	exonic	CYB5A	.		nonsynonymous SNV	CYB5A:NM_001190807:exon1:c.C14G:p.S5\
19	1863401	1863401	G	C	exonic	KLF16	.		synonymous SNV	KLF16:NM_031918:exon1:c.C96G:p.P32P
19	17476219	17476219	G	A	exonic	PLVAP	.		nonsynonymous SNV	PLVAP:NM_031310:exon3:c.C1055T:p.A352
19	24010155	24010155	T	A	exonic	RPSAP58	.		synonymous SNV	RPSAP58:NM_001355283:exon4:c.T192A:p.
19	36212267	36212267	C	T	exonic	KMT2B	.		nonsynonymous SNV	KMT2B:NM_014727:exon3:c.C2018T:p.A67
19	44116806	44116806	C	T	exonic	SRRM5	.		nonsynonymous SNV	SRRM5:NM_001145641:exon1:c.C533T:p.T:
19	53056992	53056992	G	A	exonic	ZNF808	.		nonsynonymous SNV	ZNF808:NM_001363550:exon3:c.G616A:p./
19	53270118	53270118	A	G	exonic	ZNF600	.		synonymous SNV	ZNF600:NM_198457:exon3:c.T891C:p.T297
19	57876525	57876525	A	G	exonic	TRAPPC2B	.		synonymous SNV	TRAPPC2B:NM_001355204:exon2:c.A324G:
19	58265941	58265941	T	C	exonic	ZNF776	.		synonymous SNV	ZNF776:NM_173632:exon3:c.T1443C:p.I48:
20	3802796	3802796	G	A	exonic	AP5S1	.		nonsynonymous SNV	AP5S1:NM_001204446:exon2:c.G32A:p.R11
20	36640732	36640732	-	A	exonic	TTI1	.		frameshift insertion	TTI1:NM_001303457:exon2:c.1486_1487ins
20	36640733	36640733	C	A	exonic	TTI1	.		nonsynonymous SNV	TTI1:NM_001303457:exon2:c.G1486T:p.G4!
20	48479486	48479486	-	A	exonic	SLC9A8	.		frameshift insertion	SLC9A8:NM_001260491:exon9:c.783dupA:p:
20	61512476	61512476	T	A	exonic	DIDO1	.		nonsynonymous SNV	DIDO1:NM_001193369:exon16:c.A4832T:p.
22	24316559	24316559	C	G	exonic	DDT	.		synonymous SNV	DDT:NM_001084392:exon1:c.G45C:p.V15V,
22	35661554	35661554	-	A	exonic	HMGXB4	.		frameshift insertion	HMGXB4:NM_001362972:exon4:c.847dupA
22	41240842	41240842	C	T	splicing	ST13	NM_0012785899	.		.
22	50894993	50894993	G	T	exonic	SBF1	.		synonymous SNV	SBF1:NM_001365819:exon29:c.C3939A:p.G
X	53631713	53631713	C	T	exonic	HUWE1	.		nonsynonymous SNV	HUWE1:NM_031407:exon26:c.G2579A:p.R8
X	147024747	147024747	G	A	exonic	FMR1	.		nonsynonymous SNV	FMR1:NM_001185076:exon13:c.G1309A:p.E
X	153221757	153221757	C	A	exonic	HCFC1	.		nonsynonymous SNV	HCFC1:NM_005334:exon16:c.G2741T:p.G9:
X	153581382	153581382	A	G	exonic	FLNA	.		synonymous SNV	FLNA:NM_001456:exon37:c.T6189C:p.D20(

Method S1

Mutation analysis from RNA-seq

First, using RNA-seq data from PDX cells, a mutation calling was made by an analysis pipeline called CalliNGS-NF (https://github.com/CRG-CNAG/CalliNGS-NF). The VCF file resulting from the mutation calling was annotated using annovar. Then, we selected variants that were registered in the COSMIC database and had a MAF (minor allele frequency) of 1% (0.01) or less in the SNP database (1000g, gnomAD, ESP6500, ExAC, tommo35K).